PHYSICAL REVIEW E **82**, 061703 (2010)

Splay and bend elastic constants in the nematic phase of some disulfide bridged dimeric compounds

Brindaban Kundu,[1] Santanu Kumar Pal,[2,*] Sandeep Kumar,[3] R. Pratibha,[3] and N. V. Madhusudana[3,†]
[1]*Liquid Crystal Institute, Tokyo University of Science, Yamaguchi, 1-1-1 Daigaku-Dori, San-yo-Onoda, Yamaguchi Prefecture 756-0884, Japan*
[2]*Department of Chemical & Biological Engineering, University of Wisconsin–Madison, Madison, Wisconsin 53706, USA*
[3]*Raman Research Institute, C. V. Raman Avenue, Bangalore 560 080, India*

(Received 24 February 2010; revised manuscript received 25 August 2010; published 10 December 2010)

We report measurements of the temperature dependences of the splay (K_{11}) and bend (K_{33}) elastic constants of several homologues and a binary mixutre of disulfide bridged symmetric dimers made of alkoxy cyanobiphenyl monomeric units. All of them have an even number m of carbon and sulfur atoms in the linking chain and expected to have linear conformations. Both K_{11} and K_{33} alternate depending on the parity of x which is the number of carbon atoms in the alkyl chain of a *monomer*. We will refer to this as 'odd-even' effect. This effect, occurs near the nematic-isotropic transition temperature. T_{NI}, but monotonically decrease with m at lower temperatures. We argue that these results imply large rotational fluctuations of the two halves of the dimers about the S-S bond giving rise to average bent conformations near T_{NI}. At lower temperatures those conformations which can adapt better to the given curvature deformation in the medium are favored.

DOI: 10.1103/PhysRevE.82.061703 PACS number(s): 64.70.M−, 61.30.Cz, 61.30.Eb, 62.20.D−

I. INTRODUCTION

Dimeric mesogens are usually composed of two identical moieties connected by a flexible spacer like an alkyl or alkoxy chain [1]. In the isotropic phase the molecules have a bent shape on an average [2]. Although linear conformations are favored in the nematic (N) phase due to the orientational potential, they are preferred only if the number of carbon atoms m in the spacer is even, whereas for small odd values of m the dimeric molecules have a pronounced bend [1,2]. This leads to odd-even effects in several physical properties in lower homologs [2]. One of the most extensively studied series of symmetric dimers in which the odd-even effect has been investigated in detail is that of α,ω-bis(4,4′-cyanobiphenyloxy)alkanes [BCBOA; Fig. 1(a)]. In these compounds the molecules consist of two alkoxy cyanobiphenyl units with the methyl groups in their chains fused together to form the flexible spacer. These dimers do not have terminal chains [3–5] and exhibit only the nematic phase [5]. Strong odd-even effects have been seen in the nematic to isotropic (NI) transition temperature (T_{NI}) and birefringence (Δn), with the even members having much higher values than the odd members of the lower homologs [5,6]. Recently another series of compounds very similar to BCBOA except having a disulfide bridging group between the alkoxy chains connecting the two monomers has been synthesized in our chemistry laboratory [7]. The structural formulas of BCBOA and the disulfide compound S2BCBOA are shown in Fig. 1.

The S2BCBOA dimers have *only even* number of carbon atoms $2x$ in the spacer where x is the number of carbon atoms in a monomer. The total number of carbon atoms m present in the spacer unit in BCBOA takes both odd and even values, while $m=2(x+1)$ in S2BCBOA including both the carbon and sulfur atoms has only even values. Thus, all the homologs of the disulfide compounds are expected to have linear conformations in the N phase. However surprisingly, we found that many physical properties exhibit 'odd-even' effects [8] depending on the parity of x, the number of carbon atoms in the alkyl chain of a monomer. In all further discussion 'odd' and 'even‘' in the S2BCBOA dimers relate to the parity of x and the homologs are denoted by Dx. Five homologs with x varying between 6 and 10 were investigated. T_{NI} in the disulfide compounds were found to be 20–30 °C lower than those of BCBOA series, with the same values of m (varying between 14 and 22). Further the compounds with $x=9$ and 10 exhibit a smectic-A_{ic} (SmA_{ic}) phase with an intercalated structure [7], with each dimer being shared by two adjacent smectic layers. Further, the antiparallel orientation of the cyanobiphenyl moieties favored by dipolar interactions [9] resulting in a layer spacing which is more than half the molecular length generates interdigitation as well, unlike in dimers with weakly polar moieties [2]. Also D9 exhibits a re-entrant nematic (N_{r}) phase as the temperature is lowered. To bring out the 'odd-even' effect in the disulfide compounds we reproduce in Fig. 2 the optical birefringence (Δn), dielectric anisotropy ($\Delta\epsilon$), and the orienta-

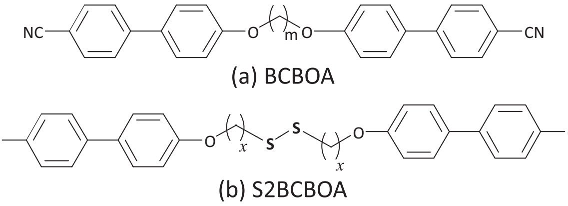

FIG. 1. Structural formulas of (a) BCBOA and their (b) disulfide bridged analogs (S2BCBOA).

---

[*] Current address: Indian Institute of Science Education and Research, Mohali MGSIPAP complex, Sector 26, Chandigarh 160019, India.

[†] nvmadhu@rri.res.in

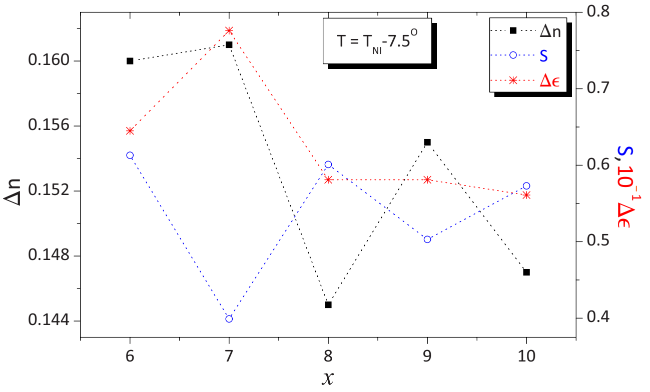

FIG. 2. (Color online) The ‘odd-even’ effects related with the parity of x, exhibited by the birefringence Δn, orientational order parameter S, and dielectric anisotropy $\Delta\epsilon$ at the shifted temperature $T-T_{\mathrm{NI}}=-7.5°$ for different homologs of the S2BCBOA series (reproduced from Ref. [8]).

tional order parameter S calculated from Δn using Hallers extrapolation technique [10] at the shifted temperature $T-T_{\mathrm{NI}}=-7.5°$, for the five homologs that were investigated.

Curiously, while the order parameter shows an ‘odd-even’ effect similar to that of T_{NI} (see Table I), with the homologs with ‘even’ x having higher values than those with ‘odd’ x, both Δn and $\Delta\epsilon$ exhibit ‘odd-even’ effects with exactly opposite trends. These unusual results can be understood by recognizing that rotational motion about the central S-S bond does not encounter any potential-energy maxima, unlike in the case of H_2C-CH_2 bond with the two projecting C-H bonds attached to each carbon atom. The linear conformation in the N phase ensures that the S-S bond is essentially along the ‘long axis’ of the director for an ‘even’ homolog, while there is a large angle between the two in an ‘odd’ dimer (Fig. 3).

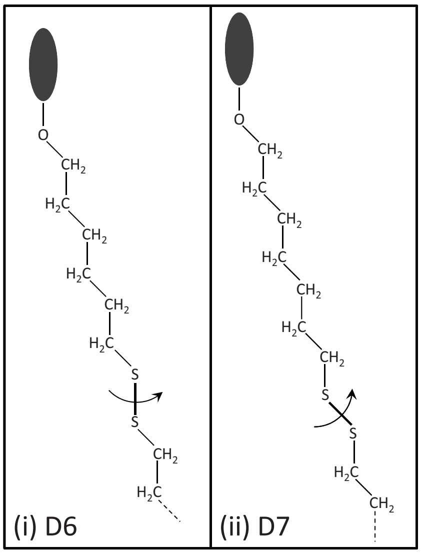

FIG. 3. The conformation of the chains in the dimers D6 and D7 in the all-trans configuration. The lower parts of the molecules are not shown to save space. Shaded ellipses correspond to the cyanobiphenyl groups. The ‘long axes’ of the molecules are vertical in both cases. The S-S bond is oriented parallel to the long molecular axis in D6, while it makes a large angle in D7. Arrow indicates a facile rotation of the two monomers of the dimer around the S-S bond (reproduced from Ref. [8]).

The facile rotation about the S-S bond increases the overall flexibility of a given S2BCBOA homolog compared to that of a BCBOA homolog with the same value of m. This lowers T_{NI} of the former especially for the ‘odd’ homologs which can develop a large bend of the structure about the S-S bond. Indeed, as will be described later, the minimum-energy conformations of single dimeric molecules bring out this essential difference between the two types of molecules. The order parameter of the ‘odd’ dimer is lower than that of a neighboring ‘even’ dimer. On the other hand, the rotations of the cyanobiphenyl monomer moieties about the S-S bond contribute better to $\epsilon_{\parallel}$, thus increasing $\Delta\epsilon$ of the ‘odd’ homolog. The C-S bonds which have relatively large polarizabilities and are oriented along the ‘long axes’ (Fig. 3) contribute to the enhanced values of Δn in the ‘odd’ homologs [8]. D7, the shortest ‘odd’ homolog studied, exhibits the largest dependences on temperature of both Δn and $\Delta\epsilon$ as the all-trans conformation depicted in Fig. 3 is closer to reality for the lower homologs than for the higher homologs which have increased flexibility of the chains. Indeed T_{NI} of D7 (with $m=16$) is lower by 40° compared to the BCBOA compound with the same value of m (see Fig. 2 in Ref. [8]).

TABLE I. Phase-transition temperatures of the different dimers and the mixture of D6 and D10.

Sample	T_{NI} (°C)	T_{AN} (°C)	$T_{\mathrm{N_rA}}$ (°C)
D6	126.8		
D7	112.2		
D8	116.1		
D9	107.6	84.9	70.0
D10	108.7	101.1	
Mixture (94% D10+6% D6)	109.4	97.2	80.4

The curvature elastic constants of nematic liquid crystals are influenced by the orientational order, shape, and conformation of the molecules as well as smecticlike short-range order. In the mean-field approximation the curvature elastic constants are proportional to S^2 far from the transition into the smectic phase, if any [11]. The elastic constants usually increase as the temperature is lowered. In the case of rodlike molecules the bend elastic constant K_{33} is usually larger than the splay elastic constant K_{11}. It can be expected that bent molecules can fit in well in a nematic with a bend distortion, thus lowering K_{33} as has been observed experimentally [12]. There have been some experimental and theoretical studies on the elastic constants of dimeric compounds whose conformations change from linear to bent depending on the number of carbon atoms in the spacer unit [13–16].

The bend elastic constant K_{33} has been found to be significantly smaller for a given odd homolog compared to that of a neighboring even homolog [13,14,16]. Only the splay elastic constants have been measured in several homologs of the prototype dimeric compound BCBOA and the expected odd-even effect has been observed [17]. The even dimers have higher values of K_{11} than the odd dimers reflecting the trend in the order parameter S, and K_{11} increases with increasing length of the dimers for $m \geq 4$ (see the inset of Fig. 13). It is of obvious interest to measure the elastic constants of the S2BCBOA dimers which exhibit monomer chain-length-dependent 'odd-even' effects in several physical properties [8] as mentioned earlier, in spite of having only linear conformations in the nematic phase.

In this paper we present our results on measurements of the splay and bend elastic constants K_{11} and K_{33} in five homologs of S2BCBOA. In addition a mixture of the homologs with $x=6$ and 10 in which the range of the re-entrant nematic phase is enlarged in comparison with that of D9 has also been studied. Close to T_{NI} we find 'odd-even' effects in both K_{11} and K_{33}, depending on the parity of x. Both K_{11} and K_{33} of D7 tend to saturate at lower temperatures in the nematic range. We discuss the results on the basis of the relative ease of rotations about the central S-S bond of the dimers. K_{33} of D9, D10, and the mixture diverge as the N-SmA_{ic} and N_{r}-SmA_{ic} transition temperatures are approached. We have also measured the entropy of the NI transition of the disulfide bridged dimers. We compare these data with those of BCBOA for the sake of completeness.

II. THEORETICAL BACKGROUND

In this section we briefly review the theoretical background of the experimental technique and the data fitting procedure used in the measurement of the splay and bend elastic constants. The elastic constants are measured by the Freédericksz transition technique [18] in which the director of a oriented sample is distorted under the application of an external field [19]. Consider a liquid-crystal cell made of two conducting glass plates with the director oriented parallel to the X axis (Fig. 4) before the application of the field. If the dielectric anisotropy ($\Delta\epsilon = \epsilon_{\parallel} - \epsilon_{\perp}$) of the liquid crystal is positive, by application of an electric field E along the Z axis, the dielectric energy is decreased by a tilting of the director. The tilt angle $\phi(z)$ is a function of the coordinate Z beyond the threshold voltage.

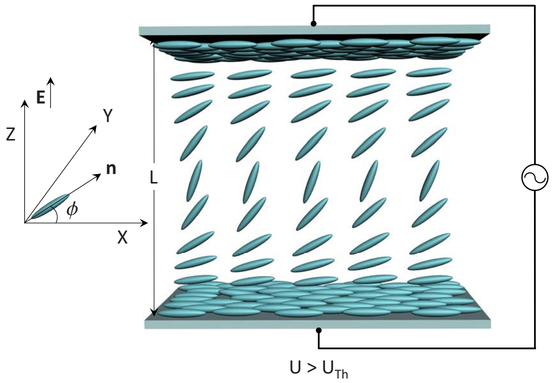

FIG. 4. (Color online) Schematic diagram illustrating director distortion under an applied electric field.

The total bulk free energy per unit area of the cell is given by [19]

$$G = \frac{1}{2}\int_0^L \left\{ (K_{11}\cos^2\phi + K_{33}\sin^2\phi)\left(\frac{d\phi}{dz}\right)^2 - \mathbf{E}\cdot\mathbf{D} \right\} dz, \tag{1}$$

where L is the thickness of the sample. The first and second terms in the integrand are due to the elastic and dielectric energy densities, respectively. **E** and **D** are the electric and displacement fields, respectively. The bulk free energy is minimized using the Euler-Lagrange equation. Assuming strong anchoring, the boundary conditions are $\phi(0)=\phi(L)=0$. The maximum distorted angle at the center is $\phi(L/2)=\phi_m$, where $d\phi/dz=0$. The applied voltage U is given by [19]

$$\frac{U}{U_{Th}} = \frac{2}{\pi}\sqrt{1+\gamma\sin^2\phi_m}\int_0^{\pi/2}\left[\frac{(1+\kappa\sin^2\phi_m\sin^2\psi)}{\mathcal{F}(\psi)}\right]^{1/2} d\psi, \tag{2}$$

where $\mathcal{F}(\psi)=(1+\gamma\sin^2\phi_m\sin^2\psi)(1-\sin^2\phi_m\sin^2\psi)$, $\kappa=(K_{33}-K_{11})/K_{11}$, $\gamma=(\epsilon_{\parallel}-\epsilon_{\perp})/\epsilon_{\perp}$, and

$$U_{Th} = \pi\sqrt{\frac{K_{11}}{\epsilon_0\Delta\epsilon}} \tag{3}$$

is the Freédericksz threshold voltage.

The optical phase difference $\delta\Phi(U)$ above $U=U_{Th}$ is a function of the applied voltage and is given by

$$\delta\Phi(U) = 2\pi\frac{n_e L}{\lambda}\left[\frac{\displaystyle\int_0^{\pi/2}\sqrt{\frac{(1+\gamma\sin^2\phi_m\sin^2\psi)(1+\kappa\sin^2\phi_m\sin^2\psi)}{(1-\sin^2\phi_m\sin^2\psi)(1+\nu\sin^2\phi_m\sin^2\psi)}}\,d\psi}{\displaystyle\int_0^{\pi/2}\sqrt{\frac{(1+\gamma\sin^2\phi_m\sin^2\psi)(1+\kappa\sin^2\phi_m\sin^2\psi)}{(1-\sin^2\phi_m\sin^2\psi)}}\,d\psi} - \frac{n_o}{n_e}\right], \tag{4}$$

where n_e and n_o are the extraordinary and ordinary refractive indices and $\nu=(n_e^2-n_0^2)/n_0^2$. The voltage dependence of the optical phase difference due to the director distortion can now be used to obtain κ. A nonlinear least-squares fitting of the experimental data corresponding to the variation of the optical phase difference with voltage is carried out using

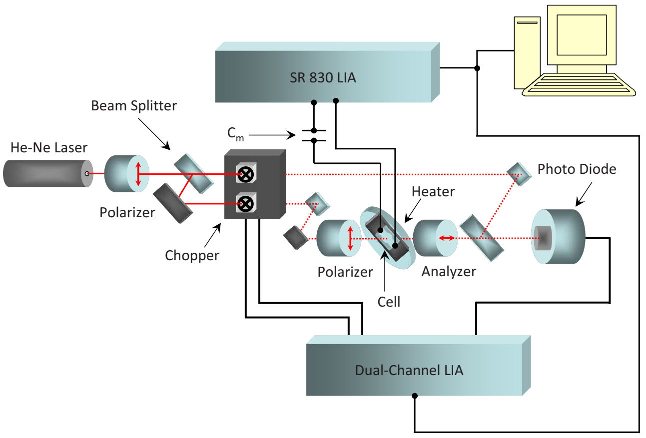

FIG. 5. (Color online) Schematic diagram of the electro-optic setup used in the measurement of the elastic constants.

Eqs. (2) and (4) and an algorithm in MATHEMATICA with ϕ_m and κ treated as adjustable parameters. The birefringence and dielectric constants which were reported in our earlier paper [8] are used in the analysis.

As the dimeric molecules can change shape under the action of splay-bend distortion, it is conceivable that the flexoelectric effect may influence the observed distortion under the external field and thus the estimation of elastic constants. Usually the nematic samples have some ionic impurities which screen the flexoelectric polarization beyond the Debye screening length. As shown by the detailed calculations of Smith *et al.* [20], the ionic charges reduce the influence of flexoelectric polarization in typical cases. In the absence of ionic species, there is a fitting degeneracy, and the bend elastic constant is reduced by ~10% if flexoelectricity is neglected in a typical case [21]. The flexoelectric coefficients of the disulfide bridged dimers have not yet been measured, and as in the earlier investigations on dimers [8] we do not take into account the influence of flexoelectricity on the measured elastic constants.

III. EXPERIMENT

An electro-optic technique in which it is possible to make both optical and electrical measurements simultaneously [12] is used for measuring various physical parameters necessary for obtaining the elastic constants. A single homogeneously aligned cell is used to obtain both the elastic constants in the nematic phase as the studied materials have positive dielectric anisotropies. The sample cell is made of two indium tin oxide coated conducting glass plates on which circular patterns are etched. Planar alignment is obtained by vacuum coating SiO at 32° grazing angle of incidence on these plates. The two plates which are separated by glass beads are placed together such that the active areas overlap and then glued together. The thickness of the empty cell is measured using an interferometric technique. The capacitance of the empty cell is measured before filling the sample. The cell with the sample is then placed in an Instec MK1 hot stage whose temperature can be controlled to an accuracy of 5 mK. The schematic of the experimental setup is shown in Fig. 5.

The beam from a He-Ne laser ($\lambda = 632.8$ nm) is initially passed through a linear polarizer and a beam splitter. Using a Perkin Elmer chopper model 198A, the two parallel beams are chopped at two different frequencies in the ratio 11:18 with mutually exclusive Fourier components. One of the beams is incident directly on a photodiode and is used as the reference beam. The other beam is directed to the same photodiode after passing through the sample placed between crossed polarizers. The sample cell is placed such that the director is at 45° to the crossed polarizers in order to get maximum sensitivity. The intensities of both the reference and sample beams are measured using a dual channel lock-in amplifier (Perkin Elmer, model 7265A), and the ratio of the sample intensity to the reference intensity is used in further analysis to take care of the source intensity fluctuations. The absolute optical phase difference ($\delta\Phi$) obtained from the transmitted intensity is used to determine the birefringence Δn. Another lock-in amplifier (Stanford Research system, model SR830) is used to make an impedance analysis of the cell at a frequency of 5641 Hz. The measured capacitance is used to obtain the perpendicular dielectric constant $\epsilon_\perp$ at a voltage of ~0.5 V, well below the Freédericksz threshold voltage. The applied voltage (U) is then varied up to ~30 V in small steps. The effective dielectric constant is determined as a function of voltage and is found to saturate at high voltages. The values corresponding to the linear part of the experimental curve are plotted against $1/U$, fitted to a straight line, and $\epsilon_\parallel$ is obtained by extrapolating to $1/U=0$. $\Delta\epsilon=\epsilon_\parallel-\epsilon_\perp$ is used in analyzing Eqs. (2) and (4). The optical phase difference $\delta\Phi$ is also simultaneously measured as a function of applied voltage, and the voltage corresponding to the Freédericksz threshold voltage is used to obtain the splay elastic constant K_{11} from Eq. (3). The ratio of the splay to bend elastic constants is obtained from the optical phase difference corresponding to the director distortion at higher voltages, using the fitting procedure. The bend elastic constant is extracted from the ratio using the value of K_{11}.

IV. RESULTS

We present the results on both the transition temperatures and the entropy of NI transition ($\Delta S/R$, where R is the gas constant) of BCBOA and S2BCBOA in Fig. 6. For the BCBOA series the odd-even effect in T_{NI} is not very prominent and ceases to exist for values of $m>18$, as the chains with large values of m have large conformational freedom and are flexible. On the other hand, the disulfide compounds exhibit a fairly prominent ‘odd-even’ effect, with the homologs with ‘even’ values of x having higher values of T_{NI}. The entropy of transition of S2BCBOA is lower than that of BCBOA with the same value of m due to the increased rotational freedom around the S–S bond in the former. The change in $\Delta S/R$ between ‘odd’ and ‘even’ members in S2BCBOA closely follows the change in S^2. In the BCBOA series, $\Delta S/R$ values continue to exhibit a strong odd-even effect unlike the NI transition temperature. In order to check the influence of the S-S linkage on the conformation of S2BCBOA, a minimum-energy conformer search was carried out using the semi-empirical method with the SPARTAN 04 package from Wave

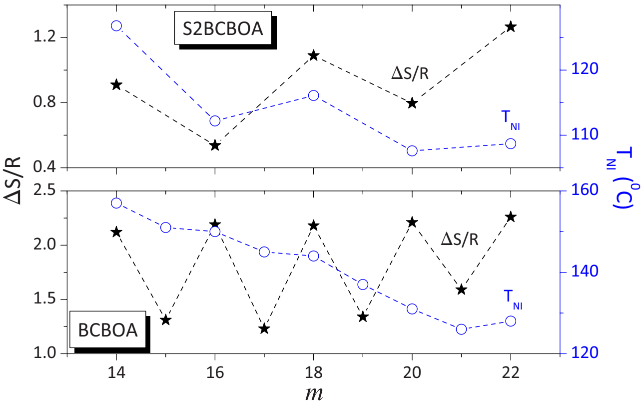

FIG. 6. (Color online) Comparison of T_{NI} and the corresponding entropy of NI transition for the homologs with m ranging from 14 to 22 for BCBOA and S2BCBOA series.

Function Inc. In Fig. 7 we show the minimum-energy conformers for homologs of BCBOA and S2BCBOA with the same value of m (=14). In the case of BCBOA, the all-trans conformation of the alkyl chain is favored and the molecule is nearly linear in shape, whereas in the case of S2BCBOA rotation around the S-S bond gives rise to a pronounced bend in the structure.

The phase-transition temperatures of the homologs D6, D7, D8, D9, D10, and the mixture used in this study are also shown in Table I. As mentioned earlier, the homologs D6, D7, and D8 exhibit only the N phase while D9 and D10 exhibit the N and SmA_{ic} phases. D9 also exhibits the reentrant nematic (N_r) phase. The range of the N_r phase is very small, and the sample tends to crystallize as the temperature is lowered in the N_r phase. We have therefore prepared a mixture of 94 mol % of D10 and 6 mol % of D6 to obtain a larger temperature range of ~8° of the N_r phase. The birefringence and dielectric data of the five pure homologs have already been reported in an earlier paper [8]. A typical experimental variation of the optical phase difference along with the theoretical fit is shown in Fig. 8. As SiO coated conducting glass plates were used to avoid pretilt, the Freédericksz transition is sharp. An attempt to incorporate finite anchoring in the fitting procedure was initially made. However, the fitting with the theoretical model was much better when the anchoring energy was assumed to be infinite, producing both the sharp Freédericksz transition as well as a good fitting in the nonlinear part. Taking into consideration the errors in the measurement of thickness of the cells and the dielectric constants the estimated error in the measurement of the elastic constants is ~5%.

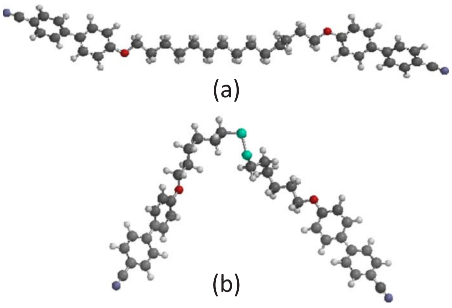

FIG. 7. (Color online) Minimum-energy conformers for (a) BCBOA and (b) S2BCBOA with $m=14$ obtained using the semiempirical method of the SPARTAN package of Wave Function. Note that the BCBOA with only alkyl chains has an essentially linear conformation, and the S-S linkage in S2BCBOA produces a pronounced bend.

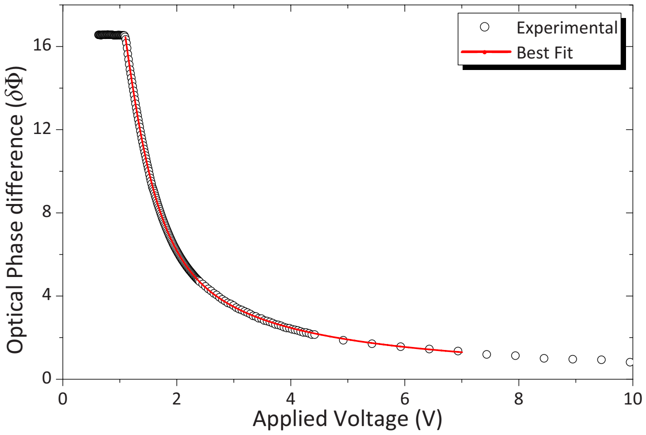

FIG. 8. (Color online) Illustration of the nonlinear least-squares fitting of the variation of optical phase difference with applied voltage for the sample D7 at the temperature $T=109$ °C.

The splay elastic constants K_{11} of all the five homologs are shown as functions of shifted temperature ($T-T_{\mathrm{NI}}$) in Fig. 9. We note the following features: (1) A clear 'odd-even' effect is seen close to T_{NI} (say at $T_{\mathrm{NI}}-5°$), with the 'even' homologs having higher values of K_{11} than the neighboring 'odd' homologs (see also Fig. 13). (2) D6, the lowest homolog studied, is known to have a weak first-order nematic-nematic transition at $T_{\mathrm{NI}}-6.3°$ as evidenced from both optical birefringence and dielectric studies [8]. The elastic data have been collected at close intervals of temperature around the N-N transition point (Fig. 9), but no signature of the N-N transition is seen in the K_{11} data, which exhibits a smooth variation around this temperature. (3) D7, the lowest 'odd' homolog studied, has the steepest variation of K_{11} with temperature as it is cooled from T_{NI}. Indeed of the five ho-

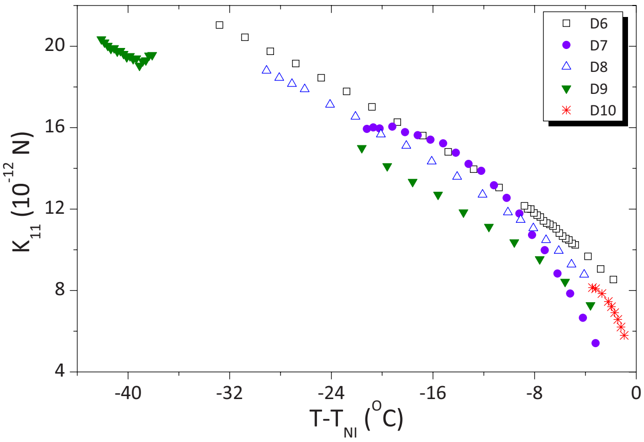

FIG. 9. (Color online) Temperature variations of the splay elastic constant K_{11} of the homologs D6–D10.

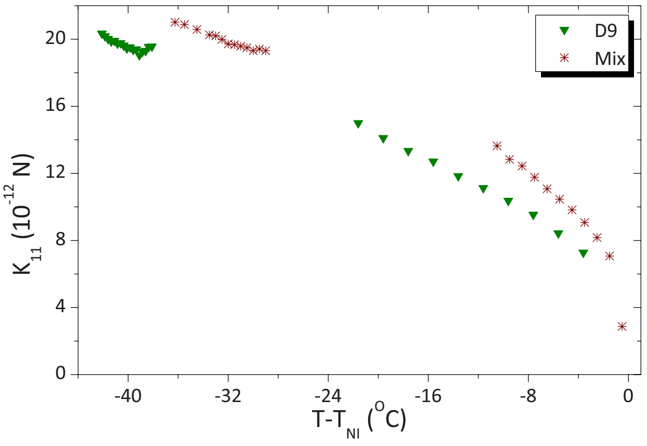

FIG. 10. (Color online) Temperature variations of the splay elastic constant K_{11} of D9 and the mixture which exhibit the N-SmA_{ic}-N_r sequence on cooling.

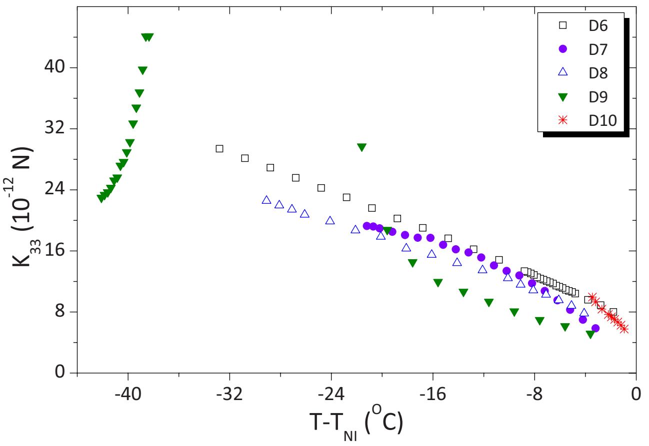

FIG. 11. (Color online) Temperature variations of the bend elastic constant K_{33} of the homologs D6–D10.

mologs, D7 has the lowest value of K_{11} at $T_{NI}-4°$, but raises to the highest value at $T_{NI}-15°$. The rate of increase decreases at lower temperatures, and K_{11} of D7 reaches saturation below $\sim T_{NI}-18°$. (4) The 'even' homologs D6 and D8 not only have relatively small temperature variations of K_{11} close to T_{NI}, but also the rate of temperature variation itself decreases slowly at lower temperatures in the nematic phase (Fig. 9). (5) The highest 'even' homolog studied, viz., D10, exhibits the nematic phase in a relatively small temperature range below which it goes over to an intercalated SmA_{ic} phase. The splay elastic constant of D10 exhibits a decreasing rate of temperature dependence as the N-SmA_{ic} transition temperature (T_{AN}) is approached (Fig. 9). (6) The highest 'odd' homolog studied, viz., D9, exhibits a much wider nematic range before it undergoes a transition to the smectic (SmA_{ic}) phase compared to D10. Further, D9 exhibits a small range of re-entrant nematic phase (N_r). Curiously, the rate of variation of K_{11} slowly *increases* as T_{AN} is approached from higher temperature (Fig. 9). As the temperature is lowered from T_{AN_r} to the re-entrant nematic phase, K_{11} decreases slightly before it starts to increase again. These trends show that the splay elastic constant is enhanced slightly due to the smecticlike short-range order close to both T_{AN} and T_{AN_r}. (7) The stiffening of K_{11} due to smecticlike short-range order is also noticeable in the mixture, which also exhibits a N-SmA_{ic}-N_r sequence as the temperature is lowered (Fig. 10). Again as T_{AN} is approached from the higher-temperature nematic phase on cooling and T_{AN_r} is approached from the lower-temperature N_r phase on heating, K_{11} tends to have higher values compared to those obtained from extrapolations of the variations in the relevant data far away from the transition temperatures.

The temperature variations of the bend elastic constant K_{33} of all the homologs studied are shown in Fig. 11. There is a broad similarity in the results with those on K_{11}, except near the transition temperature to the SmA_{ic} phase. Again, the data on D6 vary smoothly across the N-N transition point. Close to T_{NI}, D7 exhibits a relatively large temperature dependence which progressively decreases as the temperature is lowered. D9 has the lowest values of K_{33} for $T_{NI}-T$ in the range of $4°-18°$. K_{33} of this compound sharply increases, exhibiting a divergent trend as T_{AN} is approached, as the smecticlike short-range order builds up making bend distortions of the director difficult. It also exhibits a sharp divergence as the temperature is increased in the re-entrant nematic phase to T_{AN_r}. D10 exhibits only a small temperature range of the nematic phase in which K_{33} varies rapidly as this compound also exhibits the smectic phase at lower temperatures. Close to T_{NI}, K_{33} again exhibits an 'odd-even' effect, with the 'even' members having slightly higher values compared to neighboring 'odd' members. But the opposite curvature in the data on D7 and D9 lead to a monotonic decrease in K_{33} as a function of chain length between D6 and D9 for $T_{NI}-T$ lying in the range of $6°-16°$ (Fig. 11). In D9, which exhibits the re-entrant nematic phase in a relatively small temperature range, K_{33} sharply decreases as the temperature is lowered. The mixture on the other hand has a wider re-entrant nematic range and K_{33} starts to increase as the temperature is lowered after the initial sharp decrease from T_{AN_r} (Fig. 12).

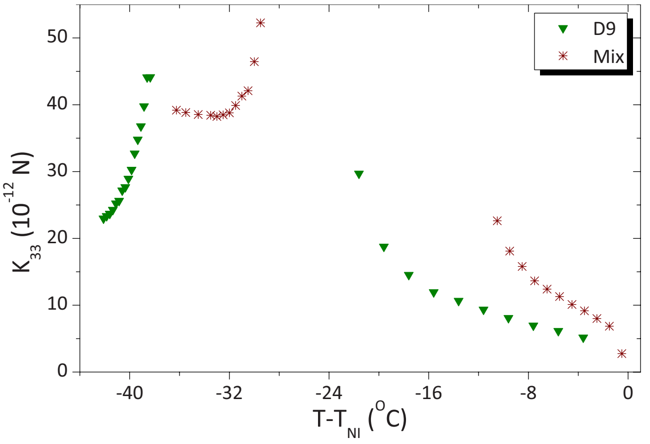

FIG. 12. (Color online) Temperature variations of the bend elastic constant K_{33} of D9 and the mixture in the nematic and re-entrant nematic phases.

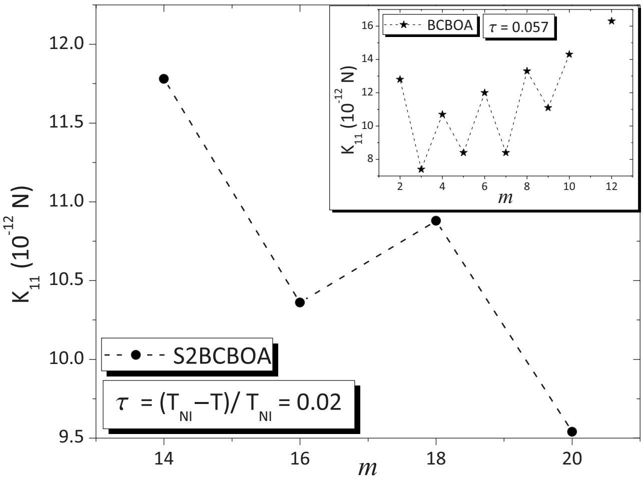

FIG. 13. Dependence of K_{11} on the spacer length of the homologs D6–D9 at a reduced temperature $\tau=0.02$. For comparison we show the dependence of K_{11} on the spacer length of the series BCBOA at the reduced temperature $\tau=0.057$ in the inset.

V. DISCUSSION

Several theoretical models have been developed to describe curvature elastic constants of nematics made of simple rodlike molecules [22,23] and those with flexible chains [24]. The curvature elasticity arises because of the orientational order in the medium, and in the mean-field approximation, $K_{ii} \propto S^2$. In a medium without any short-range order, $K_{33} > K_{11}$ [25]. However, if there is *cybotactic* layering order, which extends over only a few molecular dimensions, K_{33} can be smaller than K_{11}. On the other hand, if the nematic undergoes a *transition* to a smectic phase, smecticlike short-range order grows as T_{AN} is approached and K_{33} diverges [11]. The dimers investigated by us have an additional feature, viz., relatively flexible spacers connecting two rodlike mesogenic units. There have been some attempts to theoretically estimate the ratio of K_{33}/K_{11} for dimers with semiflexible chains and interacting with both attractive and hard rod features of the molecules [15]. The ratio was found to be considerably larger for dimers with linear conformations (i.e., with even parity) compared to those with odd parity and having bent conformations in the nematic. Experimental results are in broad agreement with this expectation [13]. Only the splay elastic constants have been measured for the BCBOA series, and at any fixed reduced temperature $\tau=(T_{NI}-T)/T_{NI}$, K_{11} exhibits alternations reflecting those of the order parameter (see the inset of Fig. 13). Further, as the spacer length m is increased beyond 3, both the odd and even homologs exhibit an increasing trend in K_{11}. In the disulfide bridged S2BCBOA dimers, 'odd-even' effects both in K_{11} and K_{33} are seen only close to T_{NI}, reflecting that in the orientational order parameter (Figs. 13 and 2). The lowest 'odd' homolog D7 exhibits a very large temperature variation in K_{11}, reflecting similar trends in both the birefringence and $\epsilon_{\parallel}$ [8]. As we argued in our earlier paper [8], the relatively short chain in D7 is stiffer than in the higher homologs, i.e., the structure shown in Fig. 3 reflects better the average conformation in the nematic phase. The thermal rotational fluctuations of the monomeric moieties about the central S-S bond lower the orientational order parameter and hence K_{11} to the lowest value near T_{NI}. As the temperature is lowered, these rotational fluctuations are reduced leading to the large increases in Δn and S as well as K_{11}. Indeed K_{11} of D7 even slightly exceeds that of D6, which is the lowest 'even' homolog at $(T-T_{NI}) \sim -10°$. Below this shifted temperature, the order parameter continues to increase as the rotational *fluctuations* are reduced. However, the temperature variation of K_{11} slows down, finally saturating below $\sim T_{NI}-18°$. The two monomeric moieties of the D7 molecule can rotate about the central S-S bond to change the *average shape* of the molecule itself, so that the "bent" molecules can be accommodated better in the static curvature deformations of both splay and bend varieties (Fig. 14), which are of course caused by the external field. Thus, both K_{11} and K_{33} of D7 tend to saturate as the temperature is lowered. This effect is of course very prominent only in D7, which has relatively short alkyl chain connected to each monomer moiety which itself stiffens at lower temperatures. Curiously at lower relative temperatures both K_{11} and K_{33} decrease *monotonically* as the chain length is increased, unlike the order parameter, which continues to exhibit the 'odd-even' effect (Figs. 2, 9, and 11). The main reason for this trend appears to be again connected with the ease of rotation of the two halves of the dimers about the S-S bond even when the alkyl chains have become stiffer at lower temperatures. Such a rotation generates nonlinear conformations of both the 'odd' and 'even' members, although the deviation from linearity is much stronger in the former case. With reference to Fig. 3 if the lower half of the D6 molecule rotates by π rad about the central S-S bond, the $C_6H_{12}SSC_6H_{12}$ chain linking the two cyanobiphenyl groups of the D6 dimer gets a bent conformation. In both types of dimers, the conformations which are more easily accommodated in a splay or bend deformation of the director field are favored at low temperatures. The increased flexibility of the alkyl chains as its length is increased in turn leads to a better accommodation of the conformation to the curvature of the director. Thus, both K_{11} and K_{33} monotonically *decrease* with chain length at low temperatures. Note that the monotonous decrease in K_{11} is exactly opposite to that found in the BCBOA series in which K_{11} increases with chain length in either the even or odd homologs (Fig. 13), bringing out the importance of the rotational freedom about the central S-S bond in the trends seen in the S2BCBOA series. Even the ratio K_{33}/K_{11} monotoni-

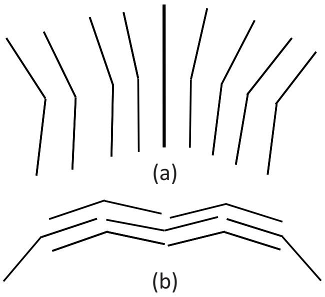

FIG. 14. Schematic drawing showing possible conformations of the dimers to accommodate (a) splay and (b) bend director fields.

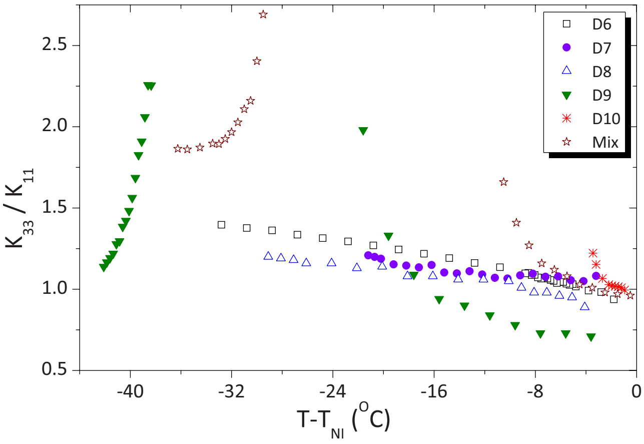

FIG. 15. (Color online) Temperature variations of the ratio of K_{33} to K_{11} in all the systems studied.

cally decreases with the increase in chain length from D6 to D9, apart from the divergence as T_{AN} is approached in D9 (Fig. 15).

Close to the nematic-isotropic transition temperature, all the homologs as well as the mixture have $K_{33}/K_{11} < 1$. This reflects the fact that the thermal rotational fluctuations about the S-S bond lead to essentially bent conformations of both the 'even' and 'odd' homologs close to T_{NI}. The absence of any signature of the *N-N* transition of D6 in both the splay and bend elastic constants indicates that the transition arises from a change in the average conformation of the chain in this case and does not influence the short-range order in the nematic. Detailed conformational energy calculations of D6 may reveal the nature of this transition. Lastly, the smectic-like short-range order which builds up close to the nematic-smectic transition temperature leads to the divergence in the K_{33} values of D9, D10, and the mixture. This simply reflects the fact that curl-**n**-type distortions are very expensive in the layered smectic phase [11]. In the dimers under investigation the smectic-A_{ic} phase has a layered structure with intercalated molecules [7]. The two cyanobiphenyl end mesogenic groups of a given dimer belong to two neighboring smectic layers. Each moiety in a given layer has an antiparallel orientation with the cyanobiphenyl end group of a neighboring dimer. The second cyanobiphenyl moiety of the latter dimer belongs to a third layer in the intercalated structure. This structure makes it difficult for the two halves of a given dimer to rotate about the central S-S bond and change its shape [see Fig. 14(a)] to be accommodated in a distorted director field, even if it is only of the splay kind. Thus, even the splay elastic constant tends to increase as the SmA_{ic} phase is approached from both the nematic and re-entrant nematic ranges (Fig. 10).

In conclusion measurements on the splay and bend elastic constants of five members of the S2BCBOA series, viz., D6–D10, and a binary mixture of D6 and D10 have shown the following interesting trends: (1) an 'odd-even' effect depending on the parity of the monomers in both K_{11} and K_{33} at temperatures close to T_{NI}. It is argued that this reflects the trend seen earlier in the order parameter and arises from the thermal rotational fluctuations about the central S-S bond of the dimer. (2) K_{33}/K_{11} is less than 1 near the nematic-isotropic transition in all the homologs, reflecting that the above thermal fluctuations essentially lead to bent conformations in both 'odd' and 'even' members. (3) The tendency for saturation of both K_{11} and K_{33} in the case of D7 and a *monotonic decrease* in K_{11}, K_{33}, and K_{33}/K_{11} as the chain length is increased, at relatively lower temperatures in the nematic range, which implies that the conformations *adapt* to the splay and bend deformations of the director field due to the ease of rotation about the central S-S bond. (4) The absence of any signature of the *N-N* transition in the K_{11} and K_{33} data of D6 unlike in the optical and dielectric data [8] implies that the transition is a reflection of a conformational change in the lowest homolog studied, which does not influence the short-range orientational order in the medium.

---

[1] A. C. Griffin and T. R. Britt, J. Am. Chem. Soc. **103**, 4957 (1981).

[2] C. T. Imrie and G. R. Luckhurst, in *Handbook of Liquid Crystals*, edited by D. Demus, J. Goodby, G. W. Gray, and H. W. Spiess (Wiley-VCH, New York, 1998), Vol. 2B, Chap. X, pp. 801–833.

[3] A. Ferrarini, G. R. Luckhurst, P. L. Nordio, and S. J. Roskilly, Liq. Cryst. **21**, 373 (1996).

[4] J. W. Emsley, G. R. Luckhurst, and G. N. Shilstone, Mol. Phys. **53**, 1023 (1984).

[5] G. R. Luckhurst, Liq. Cryst. **32**, 1335 (2005).

[6] V. N. Tsvetkov, N. V. Tsvetkov, S. A. Didenko, and V. V. Zuev, Mol. Cryst. Liq. Cryst. **265**, 341 (1995).

[7] S. K. Pal, V. A. Raghunathan, and S. Kumar, Liq. Cryst. **34**, 135 (2007).

[8] B. Kundu, S. K. Pal, S. Kumar, R. Pratibha, and N. V. Madhusudana, EPL **85**, 36002 (2009).

[9] N. V. Madhusudana and S. Chandrasekhar, Pramana, Suppl. **1**, 57 (1975).

[10] I. Haller, Prog. Solid State Chem. **10**, 103 (1975).

[11] P. G. de Gennes and J. Prost, *The Physics of Liquid Crystals*, 2nd ed. (Clarendon Press, Oxford, 1993).

[12] B. Kundu, R. Pratibha, and N. V. Madhusudana, Phys. Rev. Lett. **99**, 247802 (2007).

[13] G. A. DiLisi, E. M. Terentjev, A. C. Griffin, and C. Rosenblatt, J. Phys. II **2**, 1065 (1992).

[14] G. A. DiLisi, E. M. Terentjev, A. C. Griffin, and C. Rosenblatt, J. Phys. II **3**, 597 (1993).

[15] E. Terentjev and R. G. Petschek, J. Phys. II **3**, 661 (1993).

[16] C. Schott, S. P. Perkins, and H. J. Coles, Mol. Cryst. Liq. Cryst. **366**, 715 (2001).

[17] N. V. Tsvetkov, V. V. Zuev, I. V. Ksenofontov, and V. N. Tsvetkov, Liq. Cryst. **25**, 727 (1998).

[18] V. Fréedericksz and V. Zolina, Trans. Faraday Soc. **29**, 919 (1933).

[19] I. W. Stewart, *The Static and Dynamic Continuum Theory of*

Liquid Crystals (Taylor & Francis, London, 2004).

[20] A. A. T. Smith, C. V. Brown, and N. J. Mottram, Phys. Rev. E **75**, 041704 (2007).

[21] C. V. Brown and N. J. Mottram, Phys. Rev. E **68**, 031702 (2003).

[22] J. P. Straley, Phys. Rev. A **10**, 1881 (1974).

[23] R. G. Priest, Phys. Rev. A **7**, 720 (1973).

[24] M. Cestari, A. Bosco, and A. Ferrarini, J. Chem. Phys. **131**, 054104 (2009).

[25] P. P. Karat and N. V. Madhusudana, Mol. Cryst. Liq. Cryst. **36**, 51 (1976).